

## Near-surface VSP surveys using the seismic cone penetrometer

Kevin D. Jarvis\* and Rosemary Knight\*

### ABSTRACT

We have found that high-quality vertical seismic profile (VSP) data can be collected for near-surface applications using the seismic cone penetrometer. Cone-mounted accelerometers are used as the VSP receivers, and a sledgehammer against the cone truck baseplate is used as a source. This technique eliminates the need to drill a borehole, thereby reducing the cost of the survey, and results in a less invasive means of obtaining VSP data. Two *SH*-wave VSP surveys were acquired over a deltaic sand/silt sequence and compared to an *SH*-wave common-depth-point (CDP) reflection profile. The VSP data were processed using a combination of singular-value-decomposition filtering, deconvolution, and *f-k* filtering to produce the final VSP extracted traces. The VSP traces correlate well with cone geotechnical logs and the CDP surface-seismic data. The first breaks from the VSP can be used to generate shear-wave velocity profiles that are important for time-to-depth conversion and the velocity correction of the CDP surface data.

### INTRODUCTION

Vertical seismic profile (VSP) surveys are a means of improving the use of seismic data in obtaining information about the subsurface. In a standard VSP survey, a source at the surface generates seismic waves and receivers are deployed in an existing borehole. The receivers, which can be either downhole hydrophones or clamped geophones, are raised from the bottom of the borehole and stopped at regular intervals to record the seismic data. In most cases, the main benefit in conducting a VSP survey is the improved interpretation of surface common-depth-point (CDP) seismic data. The velocity control provided by the VSP survey allows improved accuracy in the conversion of time sections to depth sections; multiples and primary reflections can be identified and deconvolution operators designed to

eliminate the multiples. In addition, the increased bandwidth of the VSP data, compared to surface reflection data, often makes it possible to resolve smaller scale features.

VSP surveys have been extensively used in the petroleum industry (see, e.g., Gal'perin, 1974; Wuenschel, 1976; Hardage, 1985) and have been shown more recently to be a useful technique for near-surface investigations (Skvortsov et al., 1992; Milligan et al., 1997). The Milligan et al. (1997) survey was carried out in Holocene deltaic sediments (similar to the sediments in our investigation) consisting of fine silts interbedded with sand and gravel lenses. Downhole hydrophones were used to acquire VSP data over a depth range of 3 to 28 m. A multi-offset technique was used that resulted in a profile of seismic reflection data extending 9 m away from an existing borehole and with a depth range of 3 to 50 m. The bandwidth of their VSP data is significantly greater than the surface *P*-wave data acquired at the same site with usable frequencies as high as 900 Hz. The use of a 24-level hydrophone array greatly reduced the acquisition time. However, tube waves were a significant problem and were only partially eliminated by baffling the array. The development of a near-surface VSP technique which does not rely on a borehole would eliminate any problems with tube waves and result in higher quality VSP data.

The use of VSP surveys for near-surface investigations has been relatively limited. One of the reasons for this limited use is the need for a borehole to acquire the data. The drilling of a borehole significantly increases the costs associated with geophysical site characterization. In addition, there are often environmental or safety considerations such that the drilling of a borehole is not allowed. Given the significant potential value of VSP data from a site, we have investigated the acquisition of a VSP survey using a cone penetrometer. This has the advantages of reduced cost, and the cone penetrometer is generally considered to be "minimally invasive." An added benefit is the simultaneous measurement of other geotechnical parameters such as penetration resistance and friction ratio, which can then be used for stratigraphic correlations. We demonstrate the technique using a single offset *S*-wave source. However, the

Presented at the 68th Annual International Meeting, Society of Exploration Geophysicists. Manuscript received by the Editor November 10, 1998; revised manuscript received November 30, 1999.

\*Dept. of Earth and Ocean Sciences, University of British Columbia, 2219 Main Mall, Vancouver, British Columbia V6T 1Z4, Canada. E-mail: jarvis@eos.ubc.ca; knight@geop.ubc.ca.

© 2000 Society of Exploration Geophysicists. All rights reserved.

same procedure is also applicable for the acquisition of *P*-wave and multi-offset VSPs.

### GEOLOGIC SETTING

Our investigation was carried out on the Fraser River delta, southwestern British Columbia, Canada at the Kidd2 research site (Figure 1). This site has been the focus of several studies including the Canadian Liquefaction Experiment (CANLEX), which resulted in a large number of cone penetrometer holes and the retrieval of three frozen cores for laboratory measurements (Hofmann, 1997). Several hydrogeologic experiments also have been carried out at the site by using a pumping well, multilevel sampling wells, and zone-specific piezometer installations. Neilson-Welch (1999) used the multilevel sampling wells to obtain groundwater chemistry data, which were combined with measured hydrogeologic parameters to develop a groundwater flow model. The Geological Survey of Canada has obtained core, participated in geotechnical studies, and performed geophysical surveys at the site (Hunter et al., 1998) in an ongoing effort to study the liquefaction potential and earthquake site amplification effects of the Fraser delta. Based on information from these previous studies, we have developed a simple stratigraphic model involving the major lithologic units at the site: there exists a near-surface silt layer, 4–5 m thick; a sand-dominated unit, 17–18 m thick; a clayey-silt layer, 26–28 m thick; and a compact Pleistocene till. Due to the cooperation of BC Hydro, Kidd2 has become an ideal field research site where it is possible to carry out both hydrogeological and geophysical investigations.

The inset map in Figure 1 shows the acquisition grid of *SH*-wave CDP reflection data at the site with the two cone VSPs falling on one of the lines. The near-surface sediments consist of interbedded sand, silt, and clay layers, associated with the progradation of the delta during the Holocene. Underlying the deltaic sediments at a depth of approximately 50 m are Pleistocene sediments, which are composed primarily of compacted glacial till. The water table is approximately 1 m below

the surface, with some variation due to tidal influences. Because of the nearby estuary, a saltwater wedge is present within the aquifer with a depth range of approximately 12–22 m.

### CONE PENETROMETER DATA

The cone penetrometer is a technology developed by geotechnical engineers for in-situ site characterization. The basic idea is to push a steel rod with a cone-shaped tip into the ground while making measurements with sensors mounted close to the tip. The sensors, which typically consist of pressure transducers, inclinometers, thermistors, and accelerometers or geophones, are used to measure a variety of parameters such as tip resistance, sleeve friction, temperature, pore pressure, and first-arrival shear-wave velocity (Campanella et al., 1983, Robertson et al., 1986). The cone is pushed into the ground using hydraulic rams with the pushing force offset by the weight of the truck (typically 5–10 tons). The technique works extremely well in areas of alluvial and deltaic deposits consisting of clays, silts, or sands. It is not well-suited for use in gravelly sediments or rocks.

### VSP data acquisition

Two zero-offset shear-wave VSP surveys were conducted using the cone penetrometer truck from the Department of Civil Engineering at the University of British Columbia (UBC). A large sledgehammer struck against the baseplate of the truck was used as a source of *SH*-waves, and a single cone-mounted accelerometer was used as a receiver. Two records were collected with hammer blows in one direction, then two records were collected with hammer blows in the opposite direction. The records from impacts in the same direction were stacked and subtracted from each other to enhance the signal-to-noise ratio of the *SH*-waves and reduce *P*-wave interference. The data were recorded using a Nicolet oscilloscope with 15-bit data digitizing and storage capability. The depth levels at which the cone was stopped to record VSP data were

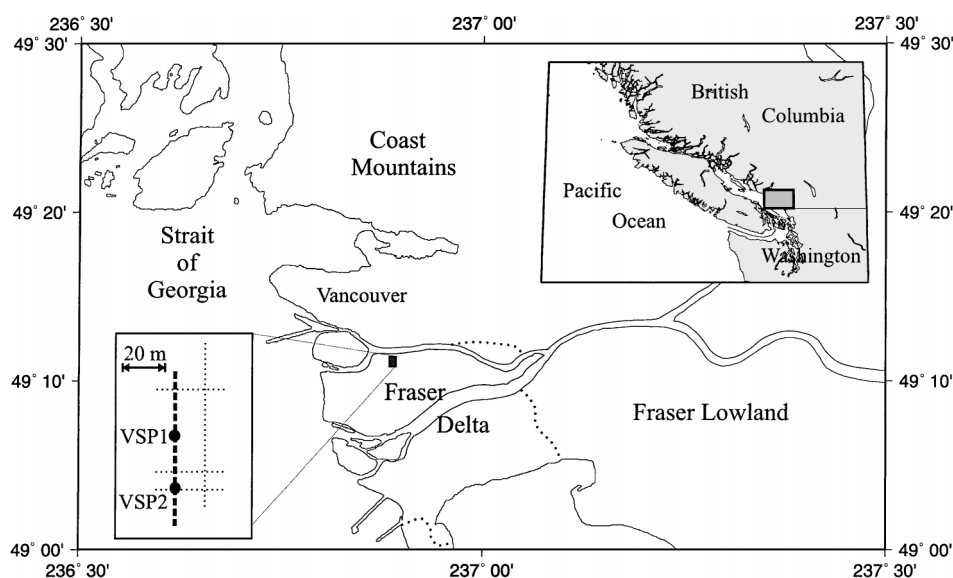


FIG. 1. Location map showing the Kidd2 research site on the Fraser River delta with the grid of *SH*-wave CDP seismic data (dotted lines) and the two VSPs (labeled VSP1 and VSP2).

chosen as a compromise between field time and spatial aliasing. The truck engine (which must be on to run the hydraulic system) was turned off before every measurement to reduce the noise.

Two VSP surveys were recorded. The first survey was conducted using a constant depth interval of 0.5 m from 3.0 m to 46.5 m, for a total of 88 traces. The second survey was performed using variable depth intervals: 0.33 m from 2.0 m to 10.0 m, 0.50 m from 10.5 m to 25.0 m and 1.0 m from 26.0 m to 49.0 m, for a total of 80 traces. The variation in depth intervals on the second survey was used as a means of reducing field acquisition time and obtaining increased coverage of the shallowest reflections.

For the VSP experiments, no modifications were made to existing instrumentation except to extend the record length. With standard cone penetrometer surveys, first arrivals are recorded to determine interval velocity, and record lengths are commonly less than 0.5 s. For the VSP survey, the record length was extended to 2 s in order to record the later arrivals. Saving data on the Nicolet oscilloscope was a time-consuming part of the operation. A digital acquisition system, using a PC-based acquisition card and software, would significantly reduce acquisition times.

An important aspect of first arrival measurements is the time and depth accuracy. Time zero, which corresponds to the instant the baseplate is struck, must be known with a very high degree of accuracy. The UBC truck is equipped with an electrical contact trigger, detailed by Robertson et al. (1986). When the metal head of the sledgehammer contacts the metal baseplate, an electrical circuit is closed which triggers the oscilloscope. Depth accuracy also determines the accuracy of calculated interval velocities. The cone truck uses 1.000-m-rod lengths, resulting in extremely accurate depths. The estimated time accuracy is  $\pm 0.03$  ms and the estimate depth accuracy is  $\pm 0.001$  m.

### VSP data processing

Data from the first cone VSP survey (referred to as VSP1) are shown in Figure 2. Data from the second cone VSP survey (VSP2) are shown in Figure 3. The first survey has two regions with a lower signal-to-noise ratio at depths of 18.0 and 31.0 m; these are attributed to sporadic instrumentation problems. The upgoing reflection from the top of the Pleistocene till is at a time of approximately 0.5 s at a depth of 3 m and 0.25 s at a depth of 46.5 m. A downgoing free surface multiple from the Pleistocene till is parallel to the first breaks with a delay of approximately 0.5 s after the first break times. The variation in trace spacing on the second survey (Figure 3) is due to the changing depth increment previously discussed. The upgoing Pleistocene till reflection can be observed in Figure 3; it is obscured at depths less than 7.0 m and most obvious between 7 and 25 m at a time of approximately 0.4 s. A downgoing free surface multiple from the Pleistocene till is not obvious on this dataset. Upgoing reflections above the Pleistocene till are not obvious in Figure 2 and Figure 3 due to the high-amplitude downgoing wavefield.

Even though both surveys were acquired at the same site, separated by only 34 m, there are considerable differences in data quality. VSP2 has a series of near-surface multiples which are not apparent in the data from VSP1. This is most obvious on the traces in the upper 7 m in Figure 3, at times greater than 0.4 s,

but the effect is also noticeable in the character of the first arrival, which is more compact on VSP1 (Figure 2). These multiples are attributed to a variation in the near-surface conditions. The surveys were done at different times of the year (VSP1 in the fall and VSP2 in the spring), so the water content of the near-surface sediments is likely to have varied. Changes in the saturation conditions of the near surface have been shown to have significant effects on the reflection character and quality

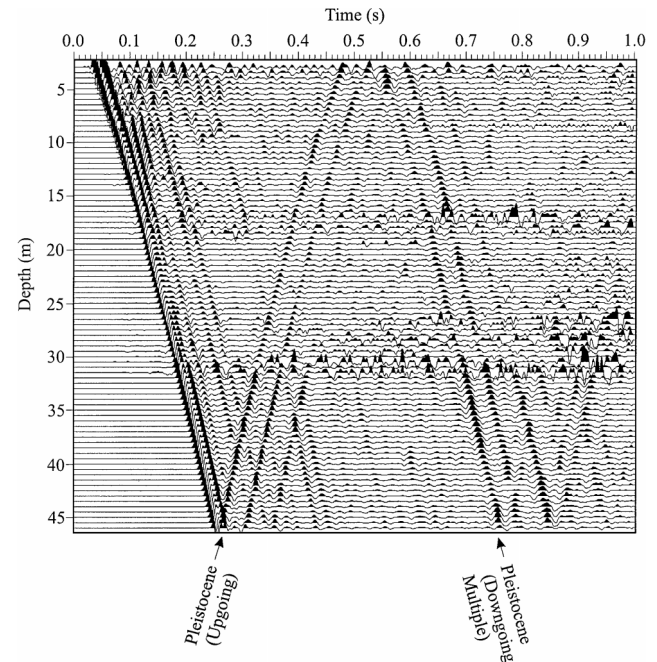


FIG. 2. Data from VSP1. A 30–150 Hz bandpass filter and spherical divergence correction have been applied to the data.

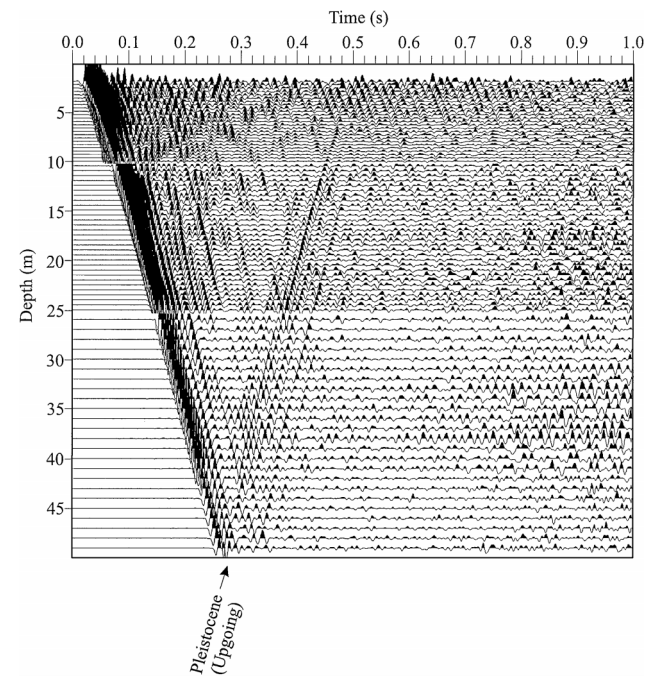


FIG. 3. Data from VSP2. A 30–150 Hz bandpass filter and spherical divergence correction have been applied to the data.

of near-surface reflection data (Jefferson and Steeples, 1995) and undoubtedly would have similar effects on VSP data. The study area also has a heterogeneous near surface with variations on the scale of meters caused by the development of the site for an electrical substation. The fill layer in the upper 2 m varies throughout the site from hard compacted till to loosely compacted sand, silt, and organic material. This likely resulted in significant differences in source and receiver coupling which thus affected the VSP data.

The differential arrival times from the direct wave first breaks were used to generate detailed interval velocity with depth functions shown in Figure 4. The determination of interval velocities using the VSP technique was an important objective of the survey. For most near-surface studies, borehole sonic logs are not available and the VSP-generated velocity profiles become critical for subsurface depth control. The estimated error in the interval velocities derived from these VSP surveys is 5%.

The processing of the two VSP datasets followed a generally accepted processing flow (as outlined by Hardage, 1985). The main objective of the processing was the separation of the upgoing and downgoing wavefields, with improvement of signal bandwidth using deconvolution. A processing flow chart is shown in Figure 5.

Compensating for spherical divergence involves a simple amplitude correction. Interval velocities from Figure 4 were used to compute a predicted amplitude decay determined by the velocity-squared time method  $[(V^2T)^{-1}]$  (Hardage, 1985), where  $V$  is the root-mean-square (rms) velocity and  $T$  is the total travelttime to a particular depth. The slope of the least-squares fit line was 1.55. An amplitude correction was applied to the data by multiplying each amplitude value by  $T^{1.55}$ .

To isolate the downgoing wavefield the singular value decomposition (SVD) technique outlined by Freire and Ulrych

(1988) was used. The downgoing wavefield was used for deconvolution and phase adjustment. Minimum phase deconvolution operators were designed based on the SVD-filtered data and applied to both the original data and the SVD-filtered data. The deconvolved SVD-filtered data were used to design match filters that were applied to the deconvolved original data. A Bracewell wavelet with frequency cutoffs of 15 and 150 Hz was chosen for the match. The match filter had the effect of removing trace-to-trace wavelet variations and reshaping the embedded wavelet to a zero-phase wavelet to allow for easy interpretation of the final results.

An  $f-k$  filter was applied to the deconvolved match-filtered data. In order to balance the trace amplitudes for the  $f-k$  filter and avoid edge effects, the direct arrivals were muted on all traces and a linear taper was applied to the top, bottom, and sides of the data. The compact first break on the data after deconvolution and match filtering did not require the application of a significant mute, thereby preserving as many data as possible. A 2-D Fourier transform of the data revealed the  $f-k$  spectrum and a pie-shaped filter (with edge tapers) was designed to isolate the aligned downgoing wavefield. The reverse transformed data were then subtracted from the input data to remove the downgoing wavefield without affecting the upgoing wavefield or background noise.

In order to flatten the upgoing wavefield, traces were shifted downwards in time by an amount equal to twice the first break

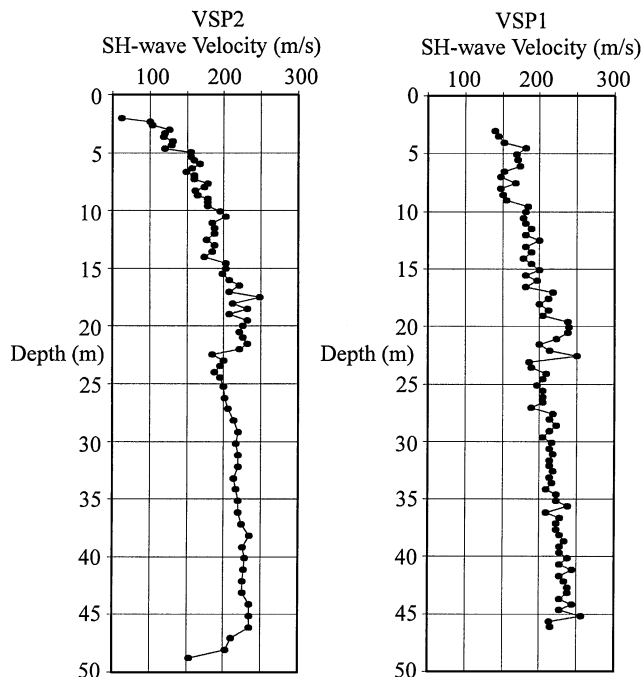


FIG. 4. Interval velocities derived from the VSP first-break arrival times.

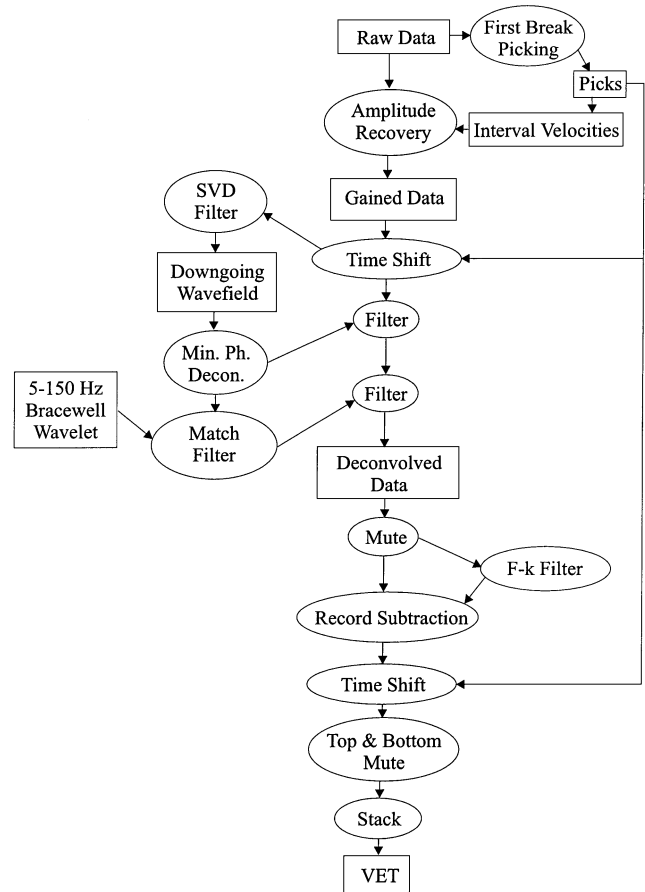


FIG. 5. Processing flow chart for the cone penetrometer VSP data.

arrival times. A top mute was designed to eliminate spurious, high-amplitude  $f$ - $k$ -filter artifacts, which tended to be generated near the initial first break times. A bottom mute was designed to remove data dominated by residual multiples and waveform changes due to attenuation (Hardage, 1985). The application of this mute is analogous to the generation of a corridor stack. A final step involved stacking the muted data to create the VSP extracted traces (VETs). The muted upgoing wavefield and VETs for the two surveys (referred to as VET1 and VET2) are illustrated in Figure 6 and Figure 7.

In Figure 7, data below 25 m were not used to generate the VET for the second survey because the deeper data were aliased. The  $f$ - $k$  spectrums clearly show that data at a sampling

interval of 1.0 m are spatially aliased at frequencies greater than 60 Hz, whereas the maximum usable frequency appears to be around 130 Hz. Deep data at a depth-sampling interval of 1.0 m were therefore not used to construct VET2. The elimination of the deeper data and the successful generation of VET2 illustrates that the cone does not necessarily have to penetrate the complete sediment column in order to obtain useful VSP information.

### Cone data acquisition

The interval velocity measurements obtained using the cone penetrometer can be used for only limited geological interpretation. This is partly due to the coarse depth sampling and also partly due to the error in the measurements, which is close to the total change in velocity associated with the different sediment types. As a result, some other independent information should be used for precise geologic calibration. This information is obtained by the other sensors installed in the cone that provide 2.5-cm sampling and are very sensitive to variations in the sediment types.

As the cone was being pushed from one VSP depth level to a deeper level, the tip resistance, sleeve friction, and pore pressure were measured. The tip resistance is a measure of the penetration force and is low in fine-grained sediments such as clay or silt and high in coarser grained material such as sand (Robertson and Campanella, 1983). The sleeve friction is a measure of the sliding friction of the cone. Geotechnical engineers have determined that the percent ratio of sleeve friction to tip resistance (referred to as the friction ratio) is a very sensitive indicator of sediment type. The friction ratio has a low, flat response in sands and a higher reading in silts and clays (Robertson and Campanella, 1983). Penetration pore pressure is relatively low in sands (hydrostatic) and higher when clay minerals are present. When the cone is stopped, dissipation of pore pressure with time can be observed. The dissipation rate aids in sediment classification and can be used to interpret the consolidation characteristics of the material (Campanella et al., 1983). Typically, measurements are made at 5-cm intervals, and the combination of tip resistance, friction ratio, and pore pressure are used to identify distinct stratigraphic sequences. These sequences are associated with interfaces which should correlate with reflections on VSP surveys.

### SH-WAVE SEISMIC REFLECTION DATA

#### Data acquisition

The CDP shear-wave seismic data were collected in June 1996 using a 24-channel Geometrics SmartSeis seismograph, 48 Geo Space horizontal geophones (20DM-28 Hz) attached to CDP spread cables, and an I/O RLS-100 roll switch. An end-on shooting configuration was used with a geophone and source spacing of 1 m, giving a far offset of 24 m and 1200% subsurface coverage. The seismic source consisted of a 35-kg steel block with metal fins attached to the base to increase the source coupling.  $SH$ -waves were generated by swinging a 5-lb (2.3-kg) sledgehammer against the sides of the block. To further increase source coupling, the block was stood upon by the person swinging the hammer.

The  $SH$ -wave technique was used to minimize mode conversions and  $P$ -wave interference. An average of 10 hammer blows

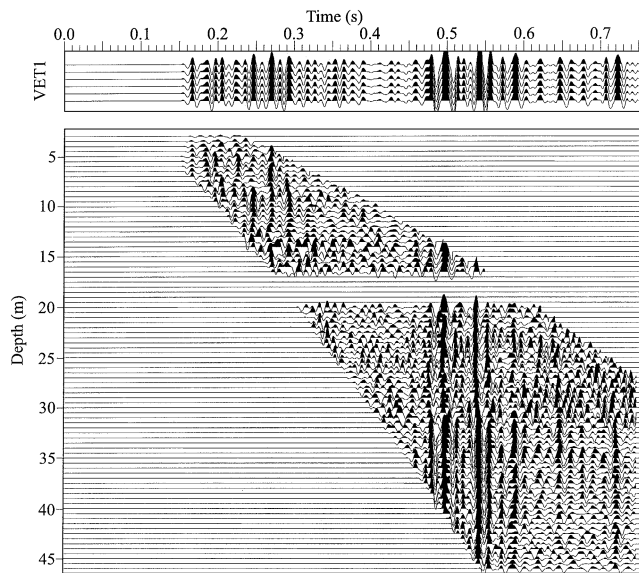


FIG. 6. Processed data from VSP1 (bottom). The upgoing wavefield has been aligned and muted. The stacked data trace is duplicated and is shown above (VET1).

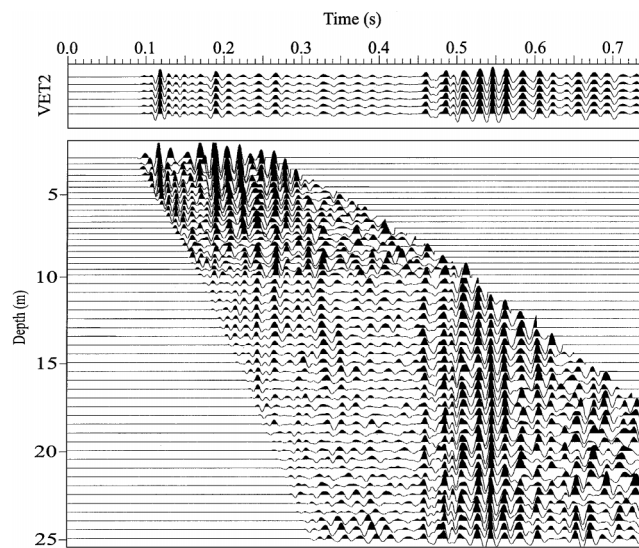


FIG. 7. Processed data from VSP2 (bottom). The upgoing wavefield has been aligned and muted. The stacked data trace is duplicated and is shown above (VET2).

were stacked for each record to improve the signal-to-noise ratio and remove the effects of the occasional misdirected blow. Data were recorded with blows in opposite directions to allow for the subtraction of the records to further reduce  $P$ -wave interference and provide additional signal-to-noise enhancement of the  $SH$ -waves. A total of five lines of  $SH$ -wave seismic data were acquired and processed, covering 420 m. The locations of these lines are shown in Figure 1. This paper only examines line 20, a 100-m north-south line (highlighted in Figure 1).

### Data processing

The seismic data were processed using ITA's UNIX-based seismic processing system installed on a Sun workstation network. The processing flow consisted of spherical divergence correction, bandpass filtering, record subtraction, deconvolution, normal moveout removal, residual statics, stacking, and migration. Refraction statics were not applied to the data because the elevation at the site varied by less than 1 m. Most of the large velocity variations in the near surface should be confined to the upper 2 m, which can be dealt with adequately by the residual statics.

A spherical divergence correction was applied using a time-scaling function with a power of 2.0. The data were bandpass filtered (25/50–150/400 Hz) using a minimum phase Butterworth filter. The record subtraction process was preceded by the application of a trace-to-trace amplitude balance. The surface consistent deconvolution used both shot and receiver gathers, with trace-by-trace editing required afterwards to remove the noisy trace segments. The elevation statics compensated for a topographic variation of less than 1 m across the site. A semblance velocity analysis was used iteratively with surface consistent residual statics. The mute function tended to be quite conservative to ensure that the amplitude variations at shallow depths did not dominate the stack. The data were migrated using an interval velocity model based on the extensive cone data available at the site, which defines the depth of key reflecting horizons.

Two shot profiles from both ends of the line are shown in Figure 8. These profiles represent the data quality after the records have been subtracted. Hyperbolic reflections are obvious at a time of 0.15 s, and a reflection from the top of the Pleistocene till is present at a time of 0.5 s. Additional reflections cannot be seen at this stage of the processing; the stacking process is needed for enhancement.

### COMPARISON OF THE GEOTECHNICAL LOGS AND VSP DATA

We obtained high-quality VSP data over a region of the subsurface where we also have cone penetrometer measurements of geotechnical parameters. The two types of data were compared to determine how each technique responds to changes in lithology and near-surface conditions. Figure 9 and Figure 10 are composite plots, which compare the geotechnical logs [friction ratio (FR), tip resistance ( $Q_c$ ), and pore pressure (U2)] with the shear wave velocity ( $V_s$ ) and the VSP data (VET1 and VET2). The interpretation of the data involves a number of factors related to the complex nature of near-surface, unconsolidated sediments or soils.

One of the dominant influences on the  $SH$ -wave velocity and tip resistance ( $Q_c$ ) is the rapid increase in effective stress in the

upper 20 m that is essentially a compaction effect. As the sediment load on a uniform sand layer increases with depth, the porosity decreases and the material becomes stiffer, thereby making it harder to penetrate and increasing the shear modulus. In Figure 9, the overall trend of increasing tip resistance from 5 MPa at 4 m to 15 MPa at 23 m is an example of the increase in penetration resistance due to compaction. In Figure 10, the velocity trend from 150 m/s at a depth of 5 m to 220 m/s at a depth of 22 m is an example of the increasing shear modulus due to compaction. Smaller scale variations within these dominant trends are possibly related to nonuniformities within the layers.

In comparing the geotechnical logs to the VSP data, it is important to recognize that the logs are sensitive to a variety of

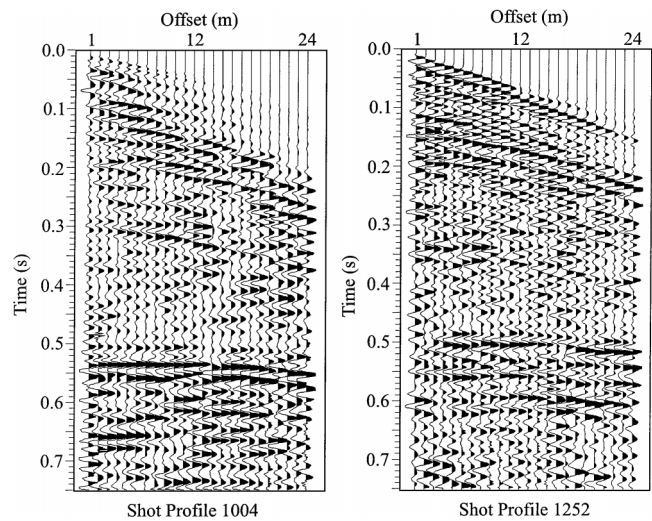


FIG. 8. Two representative shot profiles from line 20 after application of gain, trace balancing, and record subtraction. Shot profile 1004 is at the south end of the line, shot profile 1252 is at the north end.

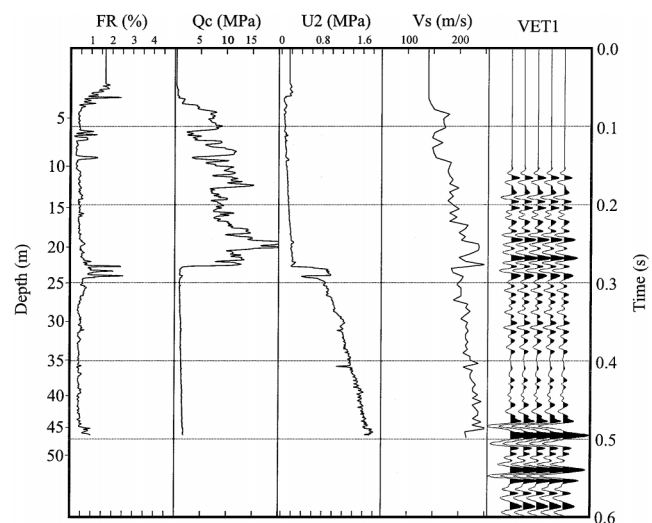


FIG. 9. Composite plot showing the relationship of the cone penetrometer friction ratio (FR), tip resistance ( $Q_c$ ), and pore pressure (U2) to the first break shear wave velocity ( $V_s$ ) and VSP1's extracted traces (VET1). The data are plotted in time with the equivalent depths indicated on the left.

physical properties, which are not necessarily related to seismic velocity or density. As a result, it is possible to observe significant changes in the geotechnical logs with no corresponding seismic reflection at that depth on the VETs. For example, the tip resistance shows large variations due to changes in sand grain size; this variation in grain size does not necessarily cause a variation in seismic velocity or density.

Civil engineers (e.g., Lunne et al., 1997) have attempted to model the cone responses in terms of specific soil conditions such as density, clay content, and grain size, but have had little success. Interpretation of the cone data is therefore accomplished using empirical relationships. Based on repeated measurements at different sites, a crossplot of friction ratio and tip resistance is used to classify soils (Campanella and Robertson, 1983). Another complexity is the fact that the cone does not fully respond to "thin" layers (Campanella and Robertson, 1983). For the standard cone used, the tip resistance will not reach a full response unless the layer is at least 36 cm thick (Campanella and Robertson, 1983). Due to these inherent complexities, we cannot expect there to be a simple relationship between the cone data and the seismic data.

The interpretation of the geotechnical logs and the VSP data is based on the stratigraphic model available for the site: a near-surface layer of silt, underlain by a sand-dominated unit, underlain by clayey silt, with the compact Pleistocene till at the base. A fine-grained silt layer near the surface (upper 4–5 m) is identified by the high friction ratio and low tip resistance. The shear wave velocity increases rapidly in this interval from 60 to 150 m/s (Figure 10). This rapid increase in velocity is most likely a compaction effect due to the high gradient in near-surface effective stress. There are no VSP data in this depth range because data were not recorded until the cone was near the base of the layer.

The zone from 5 to approximately 23 m is a sand-dominated unit. In this depth interval, the friction ratio remains low while the tip resistance shows an overall increase with depth. This

can be seen in the geotechnical data from both surveys. A significant variation in the tip resistance (most sensitive to sand grain size) is observed in both data sets in this depth interval. In this unit, we can interpret two fining-upward sequences (approximately 5–13 m and 13–22 m) within which the tip resistance decreases with decreasing depth. These two fining-upward sequences can be correlated throughout the Fraser delta (Monahan et al., 1993). The seismic propagation velocity increases within this sand layer. Most of the increase is due to the rapidly changing effective stress. There also appears to be a correlation between the zones with the highest tip resistance and those with slightly higher velocity.

Reflection events on the VETs are also identified within the sand unit. In Figure 9, VET1 shows three prominent reflections between 250 and 300 ms that are related to the lower fining-upwards sequence. The base of the sequence at a time of 280 ms correlates with a trough on VET1 and a corresponding decrease in Vs. The transition from a high-velocity to a low-velocity zone will result in a trough on zero-phase-processed seismic data. The peak on VET2 (Figure 10) at 110 ms seems to be related to the top of the coarse component of the uppermost fining-upwards sequence. A peak at 190 ms corresponds with an increase in velocity that appears to occur within a finer grained sand unit with a relatively low tip resistance. The base of the lower sequence is also represented by a trough on VET2 at a time of 260 ms.

An obvious boundary is evident on all of the geotechnical data at approximately 23 m that is a response due to the change from a sand-dominated unit to a silty unit. This silty unit has a significant amount of clay in the pore spaces. The clay component is apparent by examining the tip pore pressure plots (U2), where a large change in pore pressure is evident at a depth of 23 m. This finer grained unit is continuous down to the Pleistocene till (46.5 m for VSP1 and 49.0 m for VSP2). The tip resistance is very low in the clayey-silt unit and shows little variation. The friction-ratio, pore-pressure, and shear-wave-velocity plots show subtle variations, suggestive of variations within the silt, that are confirmed to some degree by the presence of relatively small amplitude reflections on VET1 and VET2.

The depth of cone refusal was at the top of the Pleistocene till. The VSP data were able to resolve the top of the Pleistocene till and reflections from interfaces within the till. The top of the Pleistocene till represents a change from a low-velocity clay to a high-velocity till, observed as a peak on VET1 at 495 ms and on VET2 at 505 ms. In VET2, there are a series of peaks and troughs above the Pleistocene till, starting at 460 ms that seem to correspond to a low-velocity zone, seen on the shear-wave-velocity and friction-ratio plots, which may be due to a sand or silt layer. The true nature of this layer cannot be confirmed because there is no core at this depth. The reflections within the Pleistocene till can be seen in both VET1 and VET2 down to times of approximately 0.75 s or depths of approximately 80 m. Thus, data were obtained from beyond the penetration depth of the cone; this could be extremely valuable at other sites where there is concern about contamination or hazards beyond a certain depth.

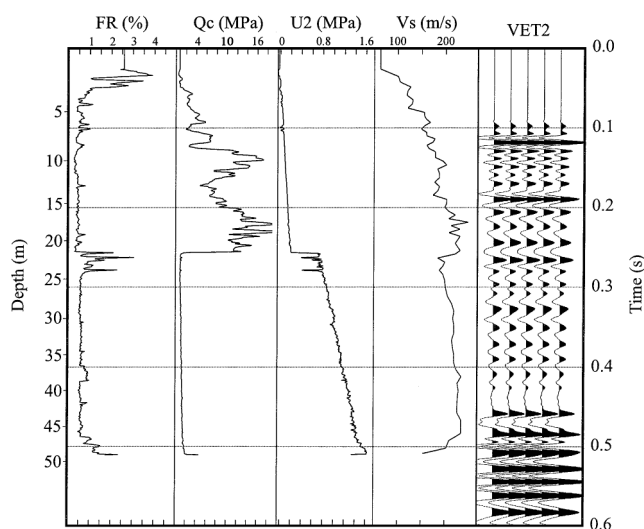


FIG. 10. Composite plot showing the relationship of the cone penetrometer friction ratio (FR), tip resistance ( $Q_c$ ), and pore pressure (U2) to the first break shear wave velocity (Vs) and VSP2's extracted traces (VET2). The data are plotted in time with the equivalent depths indicated on the left.

#### COMPARISON OF VSP AND CDP DATA

One of the main reasons for acquiring VSP data was to improve the analysis of CDP reflection data. In order to

accomplish this objective there should be a reasonable correlation between the VETs and the CDP data. Figure 11 illustrates the surface *SH*-wave reflection seismic data with the two VETs inserted at the tie points. The overall reflectivity trends compare favorably between the surface reflection data and the VSP data. The reflectivity is moderate within the sand unit, very low within the clayey silt, and high within the Pleistocene till. Individual reflections also match extremely well. The base of the lower sand sequence (at a time of approximately 270 ms) is obvious on both the CDP data and the VETs; the relative amplitudes are also comparable. The reflection from the top of the Pleistocene till at a time of approximately 500 ms also matches from the VETs to the CDP data. The top of the Pleistocene till is evident as well as a number of reflections within the till. A series of smaller amplitude reflections from 300 to 450 ms also seem to match well and are suggestive of velocity and/or density variations within the lower clayey-silt layer.

The peak at a time of 200 ms on VET2 seems to be the most significant mismatch between the VETs and the CDP data. There is no reflection on the CDP data that compares in relative amplitude. There is, however, a lower amplitude reflection on the CDP data, so it probably represents differences in the amplitude preservation of the two techniques. The CDP data were dominated by significant source-generated noise in the upper 300 ms, so the relative amplitudes are probably not well preserved. The VSP technique is not affected by this source-generated noise, so the amplitude information should be more reliable.

The higher frequency content of the VSP data is evident. The VETs show a series of distinct reflections just below the top of the Pleistocene till, whereas the same reflections on the CDP data are overlapping and complex. As has been demonstrated by other researchers (Hardage 1985; Milligan et al., 1997), this difference in frequency content allows for smaller features to be resolved in the VSP data than in the CDP data.

## CONCLUSIONS

The seismic cone penetrometer was an effective method for obtaining high-quality VSP data at the Kidd2 site. The cone VSPs have a number of advantages compared to conventional borehole VSP surveys, including decreased cost, better acoustic coupling, and the avoidance of the problems caused by tube waves. The VSP data were acquired along with other cone data, thereby providing a matched set of data for subsurface interpretation. The seismic reflectivity is well understood and limited to variations in velocity and density, whereas the cone log response is governed by additional parameters such as grain size and effective stress and relies on empirical relationships for interpretation. Subsurface velocities measured in situ are often not available for near-surface studies and are important for the processing of surface CDP seismic data as well as the accurate conversion of time to depth.

The oil and gas industry has long recognized that the analysis of VSP data can significantly improve the interpretation of reflection seismic data (Hardage, 1985). Ambiguities in the interpretation of reflection data (such as multiples) are reduced, and a precise reflectivity model can be generated to serve as the starting point for detailed seismic inversion. The inversion of seismic data based on seismic cone VSP constraints has the potential to become an effective method for characterizing the near surface.

## ACKNOWLEDGMENTS

This research was supported by an NSERC Collaborative Research Grant to Rosemary Knight. Kevin Jarvis was also supported by an NSERC postgraduate scholarship. Special thanks to Professor John Howie, who allowed us to use the UBC Department of Civil Engineering cone truck, and Golder Associates, who allowed us to use their Geometrics seismograph. The field work would not have been possible without

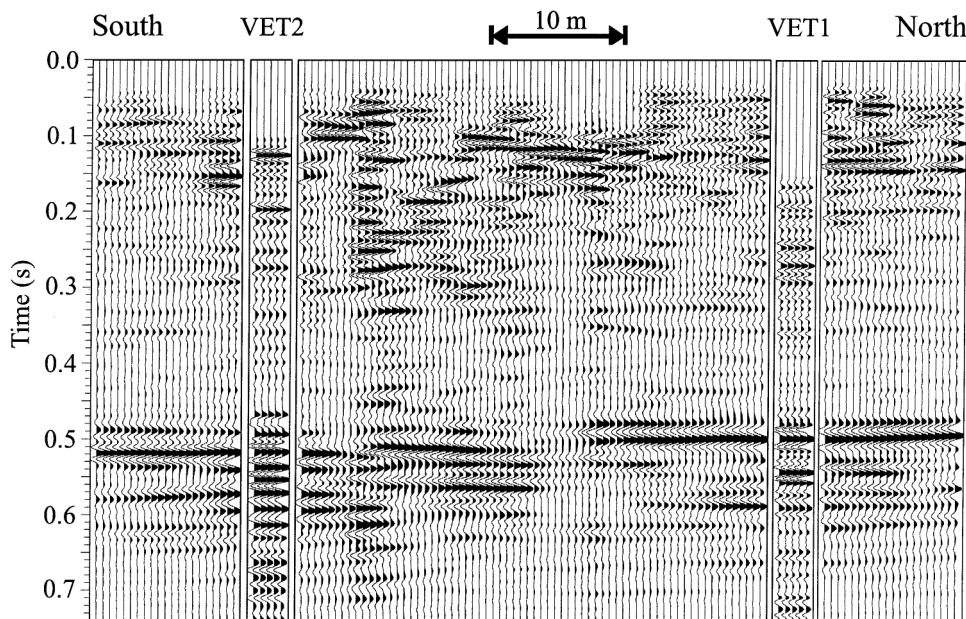


FIG. 11. *SH*-wave CDP reflection data with the extracted traces from VSP1 and VSP2 (VET1 and VET2) inserted.



the dedicated work of Chris Daniel, Heraldo Giacheti, Harald Schrempp, Scott Jackson, Richard Taylor, Paulette Tercier, Jane Rea, David Butler, and Christina Chan.

#### REFERENCES

- Campanella, R. G., Robertson, P. K., and Gillespie, D., 1983, Cone penetration testing in deltaic soils: *Can. Geotech. J.*, **20**, 23–35.
- Freire, S. L. M., and Ulrych, T. J., 1988, Application of singular value decomposition to vertical seismic profiling: *Geophysics*, **53**, 778–785.
- Gal'perin, E. I., 1974, Vertical seismic profiling: *Soc. Expl. Geophys.*
- Hardage, B. A., 1985, Vertical seismic profiling Part A: Principles, 2nd enlarged edition: Geophysical Press.
- Hofmann, B. A., 1997, In situ ground freezing to obtain undisturbed samples of loose sand for liquefaction assessment: Ph.D. thesis, Univ. of Alberta.
- Hunter, J. A., Pullan, S. E., Burns, R. A., Good, R. L., Harris, J. B., Pugin, A., Skvortsov, A., and Goriainov, N. N., 1998, Downhole seismic logging for high-resolution reflection surveying in unconsolidated sediments: *Geophysics*, **63**, 1371–1384.
- Jefferson, R. D., and Steeples, D. W., 1995, Effects of short-term variations in near-surface moisture content on shallow seismic data: 65th Ann. Internat. Mtg., Soc. Expl. Geophys., Expanded Abstracts, 419–421.
- Lunne, T., Robertson, P. K., and Powell, J. J. M., 1997, Cone penetration testing in geotechnical practice: Blackie Academic and Professional.
- Milligan, P. A., Rector III, J. W., and Bainer, R. W., 1997, Hydrophone VSP imaging at a shallow site: *Geophysics*, **62**, 842–852.
- Monahan, P. A., Luternauer, J. L., and Barrie, J. V., 1993, A delta plain sheet sand in the Fraser River delta, British Columbia, Canada: *Quaternary Internat.*, **20**, 27–38.
- Neilson-Welch, L. A., 1999, Saline water intrusion from the Fraser River estuary: A hydrogeological investigation using field chemical data and a density-dependent groundwater flow model: M.Sc. thesis, Univ. of British Columbia.
- Robertson, P. K. and Campanella, R. G., 1983, Interpretation of cone penetration tests. Part I: Sand: *Can. Geotech. J.*, **20**, 718–733.
- Robertson, P. K., Campanella, R. G., Gillespie, D., and Rice, A., 1986, Seismic CPT to measure in situ shear wave velocity: *J. Geotech. Eng.*, **112**, 791–803.
- Skvortsov, A. G., Hunter, J. A., Goriainov, N. N., Burns, R. A., Tsarov, A. M., and Pullan, S. E., 1992, High-resolution shear-wave reflection technique for permafrost engineering applications: new results from Siberia: 62nd Ann. Internat. Mtg., Soc. Expl. Geophys., Expanded Abstracts, 382–384.
- Wuenschel, P. C., 1976, The vertical array in reflection seismology—Some experimental studies: *Geophysics*, **41**, 219–232.